Journal of Molecular Neuroscience (2019) 69:166–176
https://doi.org/10.1007/s12031-019-01346-4

Involvement of A_3 Adenosine Receptor in Neuroblastoma Progression via Modulation of the Hypoxic/Angiogenic Pathway

Grazia Maugeri[1] · Agata Grazia D'Amico[2] · Concetta Federico[3] · Salvatore Saccone[3] · Salvatore Giunta[1] · Sebastiano Cavallaro[4] · Velia D'Agata[1]

Received: 8 April 2019 / Accepted: 22 May 2019 / Published online: 5 June 2019

Abstract

Neuroblastoma (NB) is the most common extracranial solid tumor of childhood. The clinical course may range from spontaneous regression towards ganglioneuroblastoma/ganglioneuroma or maturation to a very aggressive form characterized by an extensive hypoxic area. In solid tumors, extracellular microenvironment hypoxia induces the transcription of hypoxia-inducible factors (HIFs) leading to synthesis of pro-angiogenic factor, VEGF; also, it increases extracellular adenosine production from ATP breakdown. To date, the role of this nucleoside in the hypoxic/angiogenic pathway characterizing the core of cancer mass has not been investigated yet. Therefore, the aim of the present study was to analyze the adenosine effect on modulation of the HIF-1α/2α/VEGF pathway mediated through A_3 AR binding. To this end, we have used a selective A_3 AR agonist IB-MECA or antagonist VUF 5574 in an in vitro model of malignant undifferentiated and all-trans retinoic acid (RA)-differentiated SH-SY5Y cells, representing the benign form of NB. Our results have shown that specific A_3 AR stimulation induces HIF and VEGF expression through the activation of mitogen-activated protein kinase/Erk kinase signaling cascade. In conclusion, the data suggest that A_3 AR may represent a marker of NB malignancy as well as a drug target for treatment of this solid tumor.

Keywords Neuroblastoma · Hypoxia-inducible factors · Vascular endothelial growth factor · Adenosine · A_3 receptor

Introduction

Neuroblastoma (NB) represents the most common extracranial solid tumor of childhood developing from the sympathetic nervous system. It is characterized by high biological heterogeneity and variable prognosis. In some patients, it spontaneously regresses by differentiating into benign ganglioneuroma requiring no intervention whereas, in other cases, it develops in a widespread deadly metastatic tumor (Whittle et al. 2017).

✉ Velia D'Agata
vdagata@unict.it

[1] Section of Human Anatomy and Histology, Department of Biomedical and Biotechnological Sciences, University of Catania, Via S. Sofia, 87, 95123 Catania, Italy

[2] Department of Human Science and Promotion of Quality of Life, San Raffaele Open University, Rome, Italy

[3] Department of Biological, Geological and Environmental Sciences, Section of Animal Biology, University of Catania, Catania, Italy

[4] Institute of Neurological Sciences, National Research Council, Catania, Italy

NB, like other solid tumors, is characterized by extensive hypoxic areas leading to tissue necrosis and neovascularization. During tumor development, hypoxic areas expand into the cancer mass not supported by an adequate oxygen supply due to aberrant cell proliferation (Wigerup et al. 2016). The transcriptional response of cancer cells to hypoxia is represented by hypoxia-inducible factors (HIFs) comprising oxygen-stable α-subunits (HIF-1α, HIF-2α, and HIF-3α) and an oxygen-labile β-subunit, also known as aryl hydrocarbon nuclear translocator (ARNT) (Semenza 2014). By analyzing public gene expression tumor datasets, Påhlman and Mohlin (2018) have detected high HIF-1α and HIF-2α mRNA as well as extremely low HIF-3α mRNA levels in NB specimens.

In the presence of oxygen, the prolyl-4-hydroxylases (PHDs) induce the hydroxylation of α-subunits causing their degradation. Instead, under low oxygen tension levels, HIF-α proteins are stabilized by migrating to the nucleus and dimerizing with HIF-1β. This heterodimeric complex binds to hypoxia-responsive elements (HREs) which in turn regulate the expression of several genes involved in cellular differentiation, angiogenesis, apoptosis, and metastasis (Semenza 2003; Keith et al. 2011). In accord, previous studies have

demonstrated a correlation between activation of HIF-1α and the expression of CD31/PECAM1 and matrix metalloproteinases, known as biomarkers of glioblastoma aggressiveness (Musumeci et al. 2015a, b). Among HREs, vascular endothelial growth factor (VEGF) is a key player in the angiogenic process, being secreted by majority of NB cell lines and primary tumors. In particular, it is a downstream target of both HIF-1α and HIF-2α leading to aberrant new blood vessel formation with NB poor prognosis (Noguera et al. 2009).

Under hypoxia, extracellular ATP is converted to ADP and AMP, which in turn is metabolized to adenosine (Yegutkin 2014). The latter is a ubiquitous nucleoside regulating various physiological functions. Usually, its levels in body fluids range from 10 to 200 nM by drastically increasing up to 30 μM under low oxygen tension (Layland et al. 2014; Fredholm 2007).

Adenosine plays its activity binding to four subtypes of specific G protein-coupled receptors known as A_1 AR, A_{2A} AR, A_{2B} AR, and A_3 AR (Fredholm et al. 1994).

A_1 AR stimulation can stimulate adenylyl cyclase (AC), phospholipase C (PLC), calcium, or potassium channels through activation of different G proteins (Gi1, Gi2, Gi3, and G0). The A_{2A} AR coupled to Gs proteins activates AC. Instead, A_{2B} AR stimulates both AC and PLC through interaction with Gs/Gq proteins, whereas A_3 AR coupling with Gi and Gq proteins inhibits AC and stimulates PLC, respectively (Fredholm et al. 2001).

Noteworthy, the role played by A_3 AR in tumor progression under low oxygen tension has already been described in other tumors, such as human melanoma and glioblastoma (Merighi et al. 2001; Merighi et al. 2006; Gessi et al. 2010). In particular, it has been demonstrated that adenosine activates A_3 AR in response to hypoxia by increasing HIF-1α through the stimulation of the Akt or MAPK pathways (Merighi et al. 2001, 2006; Gessi et al. 2010). This event leads to VEGF stimulation triggering the aberrant vessel proliferation in tumor mass (Merighi et al. 2006, 2007).

To date, it has not been explored whether this complex mechanism is also involved in NB progression. To this end, the goal of the present work was to investigate the role of A_3 AR in the modulation of the hypoxic/angiogenic pathway in a model in vitro of malignant undifferentiated and all-trans retinoic acid (RA)-differentiated SH-SY5Y cells, representing the benign form of this tumor. Our results have shown that A_3 AR stimulation by the selective agonist IB-MECA induces HIF and VEGF expression through the activation of mitogen-activated protein kinase/Erk kinase (MAPK/ERK) signaling cascade. Furthermore, the hypoxic insult leading to angiogenic response mediated by VEGF seems to be more intense in undifferentiated as compared with RA-differentiated cells suggesting a key role of A_3 AR in NB malignancy.

Materials and Methods

Cell Culture and Differentiation

The human NB cell line SH-SY5Y, obtained from the American Type Culture Collection (ATCC) (Rockville, MD, USA), has been cultured in a mixture of 1:1 Dulbecco's modified Eagle's medium (DMEM) and Ham's F-12K Nutrient Medium supplemented with 10% of heat-inactivated fetal bovine serum (FBS), 100 U/ml penicillin, and 100 μg/ml streptomycin and incubated at 37 °C in 5% CO_2 (undifferentiated) as previously described (D'Amico et al. 2014). To realize an in vitro model of less aggressive neuroblastoma tumor, SH-SY5Y cells have been differentiated with 10 μM all-trans retinoic acid (RA) in complete growth medium (RA-differentiated) (Sigma cat no. 302-79-4) for 1 week (Maugeri et al. 2016a).

Treatments

Cells grown under hypoxia were exposed for 24 h to 100 μM desferrioxamine mesylate salt (DFX) (Sigma-Aldrich), a hypoxia-mimetic agent able to induce hypoxia by inhibiting the PHDs (Epstein et al. 2001; Hirsilä et al. 2005). This method offers the advantage to the experimentator to open the culture plate/dish/flask many times without affecting the hypoxic condition as compared with a hypoxic chamber as previously described by Maugeri et al. (2018a).

In our experiments, we used 10 μM adenosine (Sigma cat no. A9251) corresponding to endogenous concentration detected in ischemic areas (Andiné et al. 1990). The selective A_3 receptor agonist CI-IB-MECA (10 nM) [N6(3-iodobenzyl)2-chloroadenosine-5VN-methyluronamide] (Sigma cat no. I 146) or the selective A_3 receptor antagonist VUF 5574 (10 nM) N-(2-methoxyphenyl)-N′-[2-(3-pyridinyl)-4-quinazolinyl]-urea (Sigma cat no. V5888) was added to SH-SY5Y cells for 24 h in hypoxic condition. Inhibition of the MAPK/ERK signaling pathway was performed following a pretreatment of 30 min with the MEK1 inhibitor (PD98059, 50 mM; cat no. #P215, Sigma-Aldrich) as previously described by Maugeri et al. 2016b).

3-[4,5-Dimethylthiazol-2-yl]-2,5-diphenyltetrazolium Bromide Assay

The number of viable cells was evaluated using the 3-[4,5-dimethylthiazol-2-yl]-2,5-diphenyltetrazolium bromide (MTT) assay following the manufacturer's instructions (Roche), as previously described by Maugeri et al. (2018b). Cells were seeded into 96-well plates at a density of 5×10^3 cells/well in 100 μl of the culture medium in the presence or absence of RA. After 7 days, both undifferentiated and RA-differentiated cells were exposed to 100 μM DFX for 24 h.

The day after, 0.5 mg/ml of MTT (Sigma-Aldrich) was added to each well and incubated for 4 h at 37 °C. The reaction was stopped by adding 100 μl of solubilization solution; then, formazan formed by the cleavage of the yellow tetrazolium salt MTT was measured spectrophotometrically by absorbance change at 550–600 nm using a microplate reader (Bio-Rad). Six replicate wells were used for each group.

Western Blot Analysis

Proteins were extracted from total cell lysate with buffer containing 20 mM Tris (pH 7.4), 2 mM ethylenediaminetetraacetic acid (EDTA), 0.5 mM ethylene glycol-bis(β-aminoethyl ether)-N,N,N′,N′-tetraacetic acid (EGTA), 50 mM mercaptoethanol, 0.32 mM sucrose, and a protease inhibitor cocktail (Roche Diagnostics, Monza, Italy) using a Teflon glass homogenizer and then sonicated twice for 20 s using an ultrasonic probe, followed by centrifugation at 10,000*g* for 10 min at 4 °C. Protein concentrations were determined by the Quant-iT Protein Assay Kit (Invitrogen) as previously described by D'Amico et al. (2015). About 35 μg of protein homogenate was diluted in 2× Laemmli buffer (Invitrogen), heated at 70 °C for 10 min, separated on a Bio-Rad Criterion XT 4–15% Bis-Tris gel (Invitrogen) by electrophoresis, and then transferred to a nitrocellulose membrane (Invitrogen). Blots were blocked using the Odyssey Blocking Buffer (LI-COR Biosciences, Nebraska). The transfer was monitored by a prestained protein molecular weight marker (Bio-Rad Laboratories, Segrate, MI, Italy). Immunoblot analysis was performed by using appropriate antibodies: mouse anti-HIF-1alpha (cat no. NB100-105, Novus Biologicals, Littleton, CO, USA; 1:500), rabbit anti-HIF-2alpha (cat no. NB100-122, Novus Biologicals; 1:500), goat anti-VEGF (cat no. sc-1836, Santa Cruz Biotechnology; 1:200), rabbit anti-β-tubulin (cat no. sc-9104, Santa Cruz Biotechnology; 1:500) (cat no. ab37150, Abcam), rabbit anti-ADORA3 (cat no. SAB4500472, Sigma; 1:500), mouse anti-phospho Erk-1/2 (Thr202 and Tyr204 residues) (pT202/pY204.22A, cat no. sc-136521, Santa Cruz Biotechnology; 1:200), and mouse anti-total Erk-1/2 (MK1, cat no. sc-135900, Santa Cruz Biotechnology; 1:200).

The secondary antibodies goat anti-rabbit IRDye 800CW (cat no. #926-32211, LI-COR Biosciences), donkey anti-goat IRDye 800CW (cat no. #926-32214, LI-COR Biosciences), and goat anti-mouse IRDye 680CW (cat no. #926-68020D, LI-COR Biosciences) were used respectively at 1:20,000 and 1:30,000.

Blots were scanned with the Odyssey™ Infrared Imaging System (Odyssey) which is highly sensitive to reveal signals obtained from both low- and high-abundance proteins detected by chemiluminescence analysis. To quantify results in order to employ them for statistical analysis, we have performed densitometric analysis of signals on blots by using the ImageJ software, as previously described by Maugeri et al. (2017) (NIH, Bethesda, MD, USA; available at http://rsb.info.nih.gov/ij/index.html). Values were normalized to β-tubulin used as a loading control.

Immunolocalization

To determine the cellular distribution of A_3 AR and nestin proteins, immunofluorescence analysis was performed as previously described by D'Amico et al. (2017). Cells were cultured on glass cover slips, fixed in 4% paraformaldehyde in phosphate-buffered saline (PBS; 15 min at room temperature), permeabilized with 0.2% Triton X-100, blocked with 0.1% BSA in PBS, and then probed with rabbit anti-ADORA3 (1:50) and rabbit anti-nestin (1:50) antibodies. Signals were respectively revealed with Alexa Fluor 488 goat anti-rabbit for 1.5 h at room temperature (shielded from light). DNA was counterstained with 4,6-diamidino-2-phenylindole (DAPI; cat no. 940110, Vector Laboratories). After a series of washes in PBS and double-distilled water, the fixed cells were coverslipped with VECTASHIELD mounting medium (Vector Laboratories, Burlingame, USA). Immunolocalization was analyzed by confocal laser scanning microscopy (Zeiss LSM700). Green and blue signals were respectively detected with laser light at 488 nm/10 mW and 405 nm/5 mW by using the objective "Plan-Apochromat" 63×/1.40 Oil DIC M27. Each scan was individually digitalized by a high-sensitivity photomultiplier tube using the following acquisition setup: gain master, 776; digital offset, − 202; and digital gain, 1.0. All acquisitions were performed with ZEN-2010 software.

Statistical Analysis

Data are represented as mean ± standard error (SEM). One-way analysis of variance (ANOVA) was used to compare differences among groups, and statistical significance was assessed by the Tukey–Kramer post hoc test. The level of significance for all statistical tests was set at $p \leq 0.05$.

Results

Induction of HIF-1α/HIF-2α Expression by A_3 Adenosine Receptor Stimulation

To reproduce in vitro the microenvironment of the NB hypoxic area, we have treated SH-SY5Y and RA-differentiated cells with a hypoxic mimetic agent, DFX, for 12 h, 24 h, and 48 h and analyzed their viability through the MTT assay.

As observed in Fig. 1, the survival rate of RA-differentiated cells appears lower with respect to the undifferentiated group. However, these data are due to the reduced proliferation induced by RA in differentiated cells blocked in the G1 phase

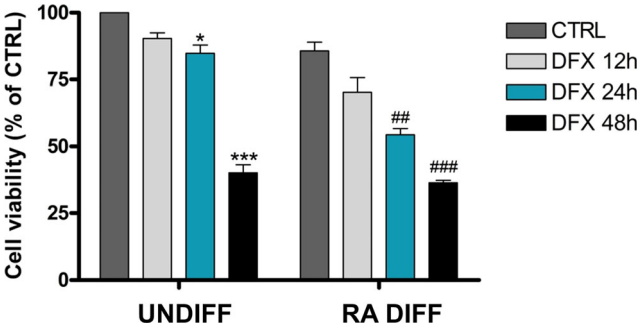

Fig. 1 Viability of undifferentiated and RA-differentiated SH-SY5Y cells exposed to hypoxia. Cell viability was evaluated on SH-SY5Y cells cultured in growth medium (undifferentiated) or added with 10 μM all-trans retinoic acid (RA-differentiated) in the presence of 100 μM DFX for 12, 24, and 48 h by the MTT assay. Results are representative of at least three independent experiments, and values are expressed as percent of CTRL. $^{*}p < 0.05$ and $^{***}p < 0.001$ vs CTRL undifferentiated; $^{\#\#}p < 0.01$ and $^{\#\#\#}p < 0.001$ vs CTRL RA-differentiated, as determined by one-way ANOVA followed by Tukey's multiple comparison test

(Qiao et al. 2012). Furthermore, DFX treatment significantly reduced cell viability in all groups as compared with the respective control ($^{*}p < 0.05$ and $^{***}p < 0.001$ vs CTRL, $^{\#\#}p < 0.01$ and $^{\#\#\#}p < 0.001$ vs CTRL SH-SY5Y + RA). In light of these results, we have decided to expose cells to 24 h of hypoxia in the next experiments since we found a relevant difference among undifferentiated (survival rate reduction of ~ 20% as compared with undifferentiated SH-SY5Y cells) and RA-differentiated cells (survival rate reduction of ~ 30% as compared with SH-SY5Y cells plus RA) treated for 24 h with DFX ($^{*}p < 0.05$ vs CTRL SH-SY5Y, $^{\#\#}p < 0.01$ vs CTRL SH-SY5Y + RA).

To confirm that RA-differentiated SH-SY5Y cells represented the benign form of NB, nestin cytolocalization has been investigated through immunofluorescence analysis. As shown in Fig. 2, the immunosignal of this marker associated with tumor aggressiveness was lower in RA-treated as compared with undifferentiated cells in either normoxia or hypoxia confirming the less malignancy of the RA-treated group.

To study the role of A_3 AR in NB progression, we have also analyzed its expression in cells grown in normoxia or hypoxia. As shown in Fig. 3a, A_3 AR levels were significantly decreased in RA-differentiated as compared with undifferentiated cells ($^{**}p < 0.01$ vs UNDIFF). Under hypoxia, it upregulated by significantly increasing in undifferentiated as compared with RA-differentiated NB cells ($^{***}p < 0.001$ vs CTRL, $^{\#\#}p < 0.01$ vs RA, $^{\$\$\$}p < 0.001$ vs DFX). This data has been also confirmed through immunofluorescence

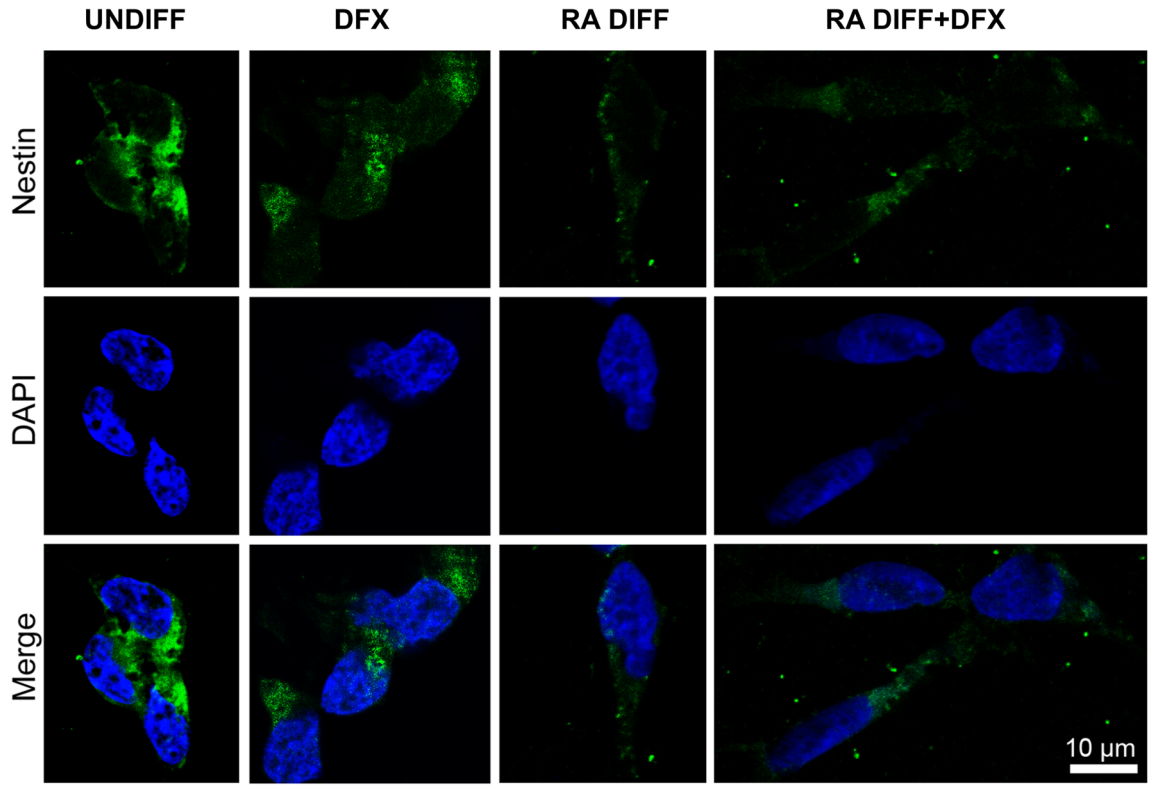

Fig. 2 Expression of nestin protein in undifferentiated and RA-differentiated neuroblastoma cells exposed to hypoxia. Representative photomicrographs show the nestin protein (green) obtained with a confocal laser scanning microscope. Cells were cultured in growth medium (UNDIFF) or added with 10 μM all-trans retinoic acid (RA DIFF) in normoxic or hypoxic condition. Photomicrographs are representative results of fields taken randomly from the slide and scanned by confocal laser scanning microscopy (CLSM; Zeiss LSM700). Nuclei were stained with DAPI (blue). Scale bar 10 μm and viewed at ×200 magnification

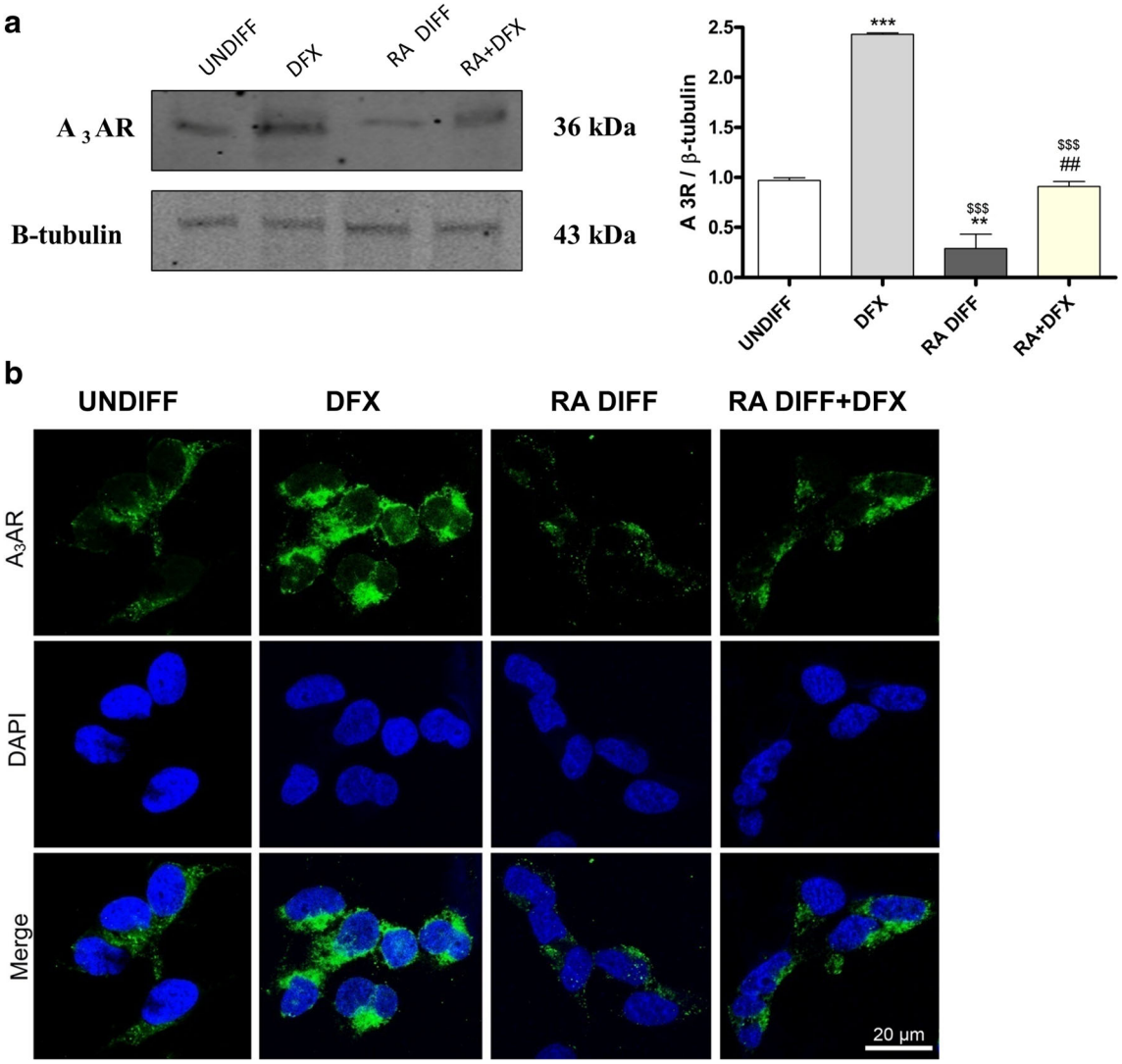

Fig. 3 Expression of A_3 receptor protein in undifferentiated and RA-differentiated neuroblastoma cells exposed to hypoxia. **a** Representative immunoblots of A_3 AR expression levels in SH-SY5Y cells cultured in growth medium (UNDIFF) or added with 10 μM all-trans retinoic acid (RA DIFF) in normoxic or hypoxic condition. The bar graphs show mean ± SEM of signals, normalized to β-tubulin expression; results from three independent experiments. $^{**}p < 0.01$ and $^{***}p < 0.001$ vs UNDIFF; $^{\#\#}p < 0.01$ vs RA DIFF, as determined by one-way ANOVA followed by the Tukey post hoc test. Relative band densities were quantified by using the ImageJ software. **b** Representative photomicrographs show A_3 AR (green) obtained with a confocal laser scanning microscope. Cells were cultured in growth medium (UNDIFF) or added with 10 μM all-trans retinoic acid (RA DIFF) in normoxic or hypoxic condition. Photomicrographs are representative results of fields taken randomly from the slide and scanned by confocal laser scanning microscopy (CLSM; Zeiss LSM700). Nuclei were stained with DAPI (blue). Scale bar 20 μm and viewed at ×100 magnification

analysis. Higher A_3 AR immunosignal has been detected in undifferentiated as compared with RA-differentiated cells exposed to hypoxia (Fig. 3b). To evaluate the effect mediated by A_3 AR on HIF expression under low oxygen tension, we have treated cells with adenosine or the selective A_3 AR agonist CI-IB-MECA alone or in combination with the selective A_3 AR antagonist VUF 5574. As shown in Fig. 4, HIF-1α and HIF-2α expression was significantly increased in undifferentiated and RA-differentiated NB cells exposed to hypoxia ($^{**}p < 0.01$ and $^{***}p < 0.001$ vs UNDIFF, $^{\#\#\#}p < 0.01$ vs RA DIFF). Treatment with adenosine or CI-IB-MECA strongly enhanced HIF-1α/2α expression although we have found higher levels in undifferentiated as compared with RA-differentiated NB cells ($^{\S}p < 0.05$ and $^{\$\$\$}p < 0.001$ vs DFX, $^{\wedge\wedge\wedge}p < 0.001$ vs RA + DFX, $^{\$\$\$}p < 0.001$ vs DFX + IB-MECA).

Co-treatment of undifferentiated and RA-differentiated cells with CI-IB-MECA and 10 nM VUF 5574 drastically reduced the expression of HIF-1α/2α, by confirming the A_3 AR selective role in hypoxic process modulation ($^{\$\$\$}p < 0.001$ vs DFX + IB-MECA, $^{+++}p < 0.001$ vs RA + DFX + IB-MECA).

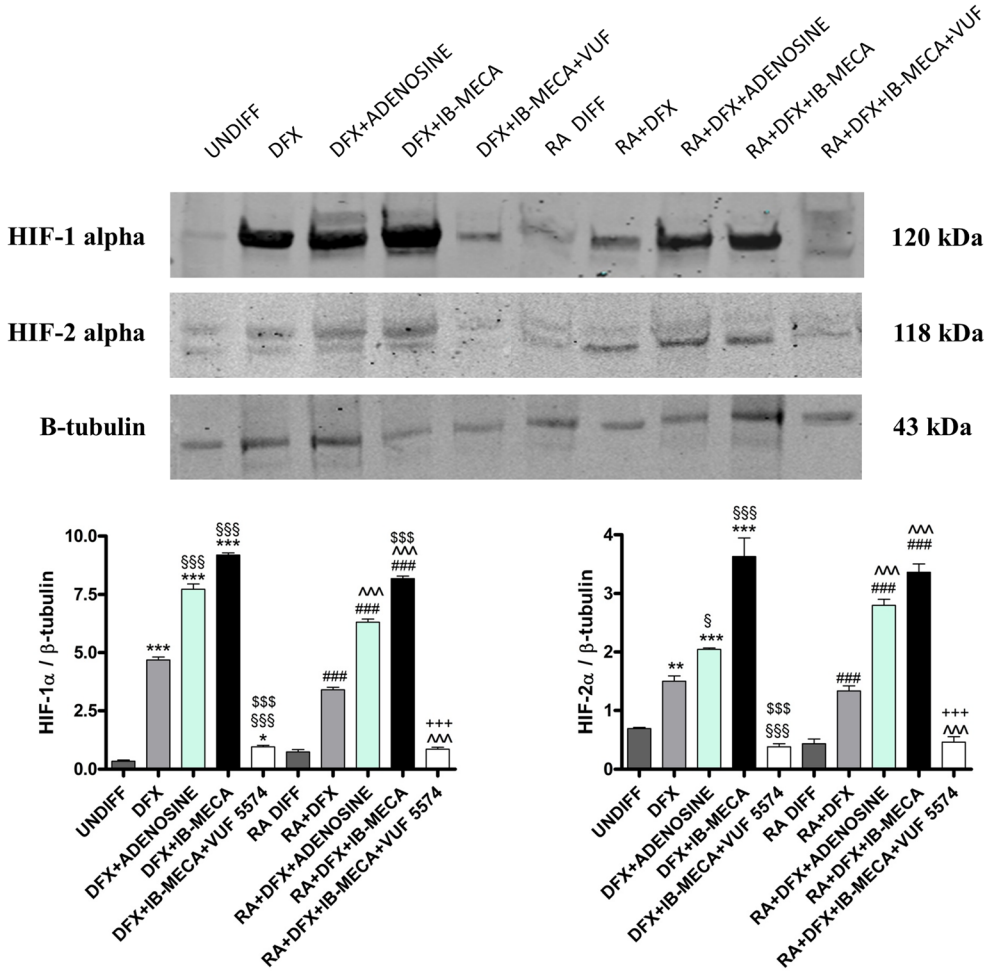

Fig. 4 Induction of HIF expression by adenosine in undifferentiated and RA-differentiated neuroblastoma cells exposed to hypoxia. Representative immunoblots of HIF-1α and HIF-2α expression levels in SH-SY5Y cells cultured in growth medium (UNDIFF) or added with 10 μM all-trans retinoic acid (RA DIFF) in normoxic or hypoxic condition treated with 100 μM adenosine or 100 nM IB-MECA alone or in combination with 10 nM of VUF 5574 for 24 h. The bar graphs show mean ± SEM of signals, normalized to β-tubulin expression; results from three independent experiments. $^{**}p < 0.01$ and $^{***}p < 0.001$ vs UNDIFF; $^{\#}p < 0.05$ and $^{\#\#\#}p < 0.001$ vs RA DIFF; $^{\S\S\S}p < 0.001$ vs DFX; $^{\wedge\wedge\wedge}p < 0.001$ vs RA + DFX, $^{\wedge\wedge\wedge}p < 0.001$ vs RA + DFX; $^{+++}p < 0.001$ vs RA + DFX + IB-MECA, as determined by one-way ANOVA followed by the Tukey post hoc test. Relative band densities were quantified by using the ImageJ software

A_3 AR Activation Mediates VEGF Expression

To demonstrate that A_3 AR activation leading to HIF-1α/2α upregulation is involved in NB aberrant angiogenesis, we have evaluated VEGF levels in untreated and RA-treated cells cultured under hypoxia with CI-IB-MECA alone or in combination with VUF 5574. As shown in Fig. 5, the selective administration of the A_3 AR agonist significantly increased the expression of VEGF in cells exposed to hypoxia ($^{\S\S\S}p < 0.001$ vs DFX, $^{\wedge\wedge\wedge}p < 0.001$ vs RA + DFX) whereas CI-IB-MECA plus VUF 5574 co-treatment drastically reduced its level in either undifferentiated or RA-treated cells ($^{\$\$\$}p < 0.001$ vs DFX + IB-MECA, $^{+++}p < 0.001$ vs RA + DFX + IB-MECA).

However, VEGF expression was significantly higher in SHSY5Y as compared with RA-treated cells during the hypoxic process, suggesting that A_3 AR mediates a more intense effect on the hypoxic/angiogenic process in undifferentiated malignant cells ($^{\$\$\$}p < 0.001$ vs DFX + IB-MECA).

A_3 AR Activation Modulates the Hypoxic/Angiogenic Process Through the Stimulation of the MAPK/ERK1/2 Pathway

To investigate whether A_3 AR activation modulates HIF expression through the stimulation of the MAPK/ERK1/2 pathway, we have treated undifferentiated and RA-differentiated NB cells exposed to hypoxia with CI-IB-MECA and PD98059, a MEK1 inhibitor. As shown in Fig. 6, PD98059 co-treatment with the A_3 AR selective agonist has significantly decreased the expression levels of both HIF-1α and HIF-2α in untreated and RA-treated cells exposed to hypoxia as

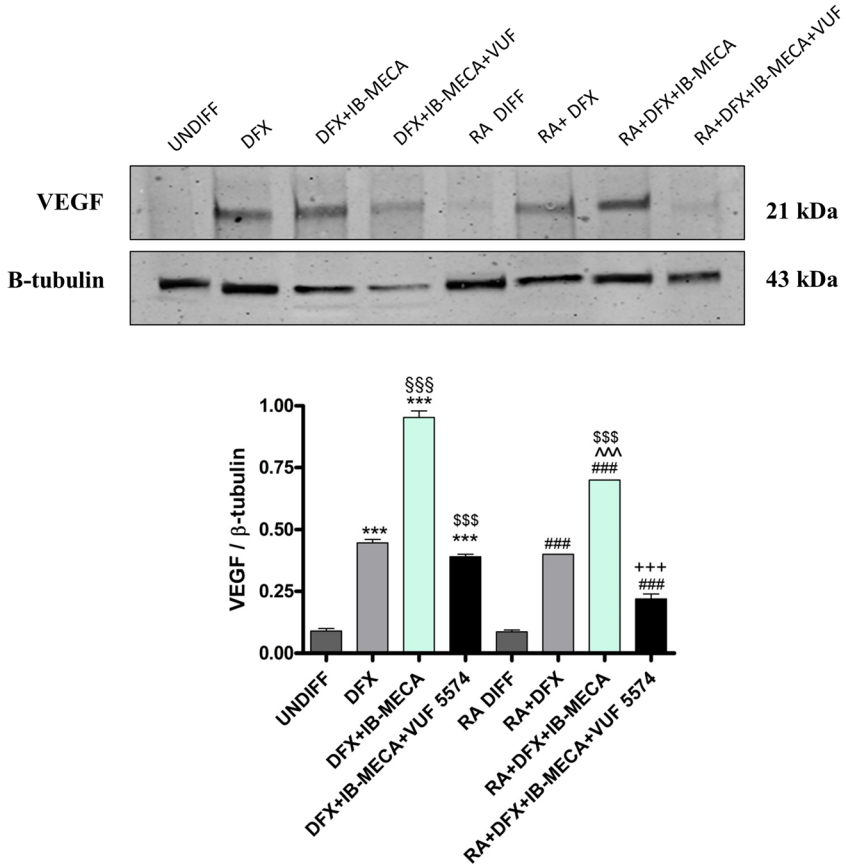

Fig. 5 Expression of VEGF from undifferentiated and RA-differentiated neuroblastoma cells exposed to hypoxia via the A_3 adenosine receptor. Representative immunoblot of VEGF expression in SH-SY5Y cells cultured in growth medium (UNDIFF) or added with 10 μM all-trans retinoic acid (RA DIFF) treated with 100 nM IB-MECA alone or in combination with 10 nM of VUF 5574 under hypoxic condition. The bar graphs show mean ± SEM of signals, normalized to β-tubulin expression; results from three independent experiments. $^{***}p < 0.001$ vs UNDIFF; $^{§§§}p < 0.001$ vs DFX; $^{\$\$\$}p < 0.001$ vs DFX + IB-MECA; $^{###}p < 0.001$ vs RA DIFF; $^{\wedge\wedge\wedge}p < 0.001$ vs RA + DFX; $^{+++}p < 0.001$ vs RA + DFX + IB-MECA, as determined by one-way ANOVA followed by the Tukey post hoc test. Relative band densities were quantified by using the ImageJ software

compared with cells cultured with IB-MECA alone ($^{\$\$\$}p < 0.001$ vs DFX + IB-MECA, $^{+++}p < 0.001$ vs RA + DFX + IB-MECA).

To confirm the MAPK/ERK1/2 pathway involvement in HIF expression mediated by A_3 AR, we analyzed the activation state of ERK1/2 in untreated and RA-treated cells exposed to hypoxia after A_3 AR agonist treatment. As demonstrated in Fig. 7, CI-IB-MECA treatment significantly increased the phosphorylation of ERK1/2 ($^{§§§}p < 0.001$ vs DFX, $^{\wedge\wedge\wedge}p < 0.001$ vs RA + DFX).

Discussion

NB prognosis differs based on the tumor stage and its biological characteristics. Subjects with low-risk disease are generally managed with surgical resection. Intermediate patients undergo surgical resection and chemotherapy, whereas the procedures for high-risk patients remain controversial needing the identification of a new therapeutic approach to improve survival (Murphy and La Quaglia 2014).

The progression of NB towards a more aggressive and metastatic phenotype is triggered by a low oxygen tension microenvironment leading to the generation of immature stem cells. Furthermore, hypoxia represents the major driving force towards tumor vascularization. VEGF, a downstream target of both HIF-1α and HIF-2α released by NB cells and other primary tumor cells, promotes endothelial cell proliferation and angiogenesis (Noguera et al. 2009).

In the last decades, several evidences have shown the involvement of adenosine in tumor progression through mediation of the immune system. In particular, this purine nucleoside, highly expressed in the hypoxic core of a solid tumor, interferes with the cancer cell recognition mediated by the cytolytic immune system (Blay et al. 1997; Merighi et al. 2003). Among the four G protein-coupled ARs, A_3 AR could

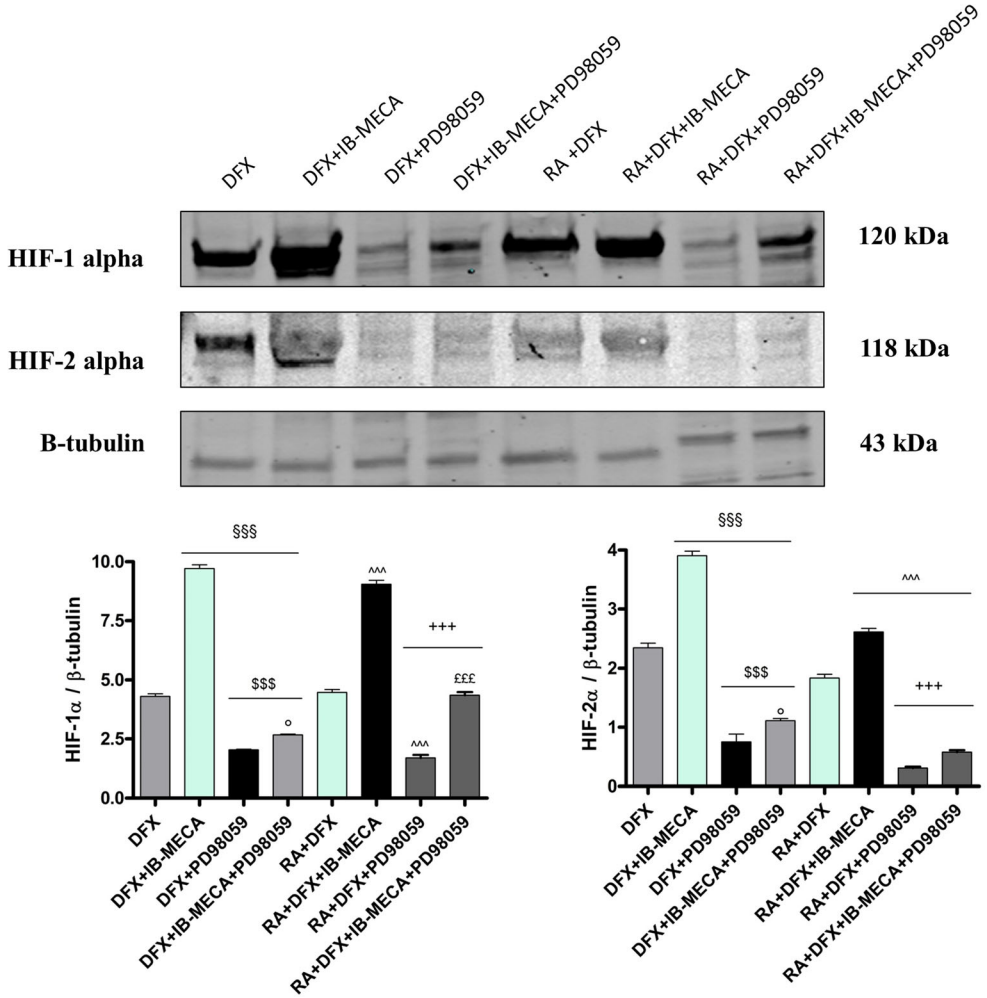

Fig. 6 A_3 adenosine receptor regulates HIF expression in undifferentiated and RA-differentiated neuroblastoma cells exposed to hypoxia through the MAPK/ERK pathway. Representative immunoblot of HIF-1α and HIF-2α expression in SH-SY5Y cells cultured in growth medium (UNDIFF) or added with 10 μM all-trans retinoic acid (RA DIFF) treated with 100 nM IB-MECA or 50 μM PD98059 alone or in combination under hypoxic condition. The bar graphs show mean ± SEM of signals, normalized to β-tubulin expression; results from three independent experiments. $^{§§§}p < 0.001$ vs DFX; $^{$$$}p < 0.001$ vs DFX + IB-MECA; $^{°}p < 0.05$ vs DFX + PD98059; $^{^^^}p < 0.001$ vs RA + DFX; $^{+++}p < 0.001$ vs RA + DFX + IB-MECA; $^{£££}p < 0.001$ vs RA + DFX + PD98059, as determined by one-way ANOVA followed by the Tukey post hoc test. Relative band densities were quantified by using the ImageJ software

be an interesting target in cancer therapy. This receptor is highly expressed in several tumors, including human malignant melanoma, mouse pineal gland tumor cells, glioblastoma, and human prostatic cells (Gessi et al. 2001; Merighi et al. 2001, 2006; Suh et al. 2001; Gessi et al. 2002; Jajoo et al. 2009). Its stimulation is involved in the control of the cell cycle. However, it seems to have either a pro- or antiapoptotic controversial role depending on the cell type (Yao et al. 1997; Nakamura et al. 2006; Gessi et al. 2007).

In the last years, more attention has been addressed towards the relationship between A_3 AR and hypoxia. Previous studies have indicated that this receptor is able to transduce extracellular hypoxic signals into the cell by increasing HIF levels through MAPK/ERK1/2 signaling cascade activation (Gessi et al. 2004; Merighi et al. 2005, 2006; Torres et al. 2019). Furthermore, its activation promotes VEGF expression, a key player in the angiogenic process of glioblastoma and colon cancer cells.

To reproduce in vitro the low oxygen tension microenvironment of the NB area, we have treated SH-SY5Y and RA-differentiated cells with a hypoxic mimetic agent, DFX. This salt acts through the chelation of Fe^{2+} bound to the active site of PHD, involved in HIF-1 degradation. The increased level of the latter regulates the oxygen supply to tissue and cells by decreasing the activity of its major consumers, mitochondria (Okamoto et al. 2017). Here, we have demonstrated for the first time the involvement of A_3 AR in NB progression via modulation of the hypoxic process. We have found high expression of A_3 AR following hypoxic insult, particularly in undifferentiated rather than RA-treated SH-SY5Y cells (Fig.

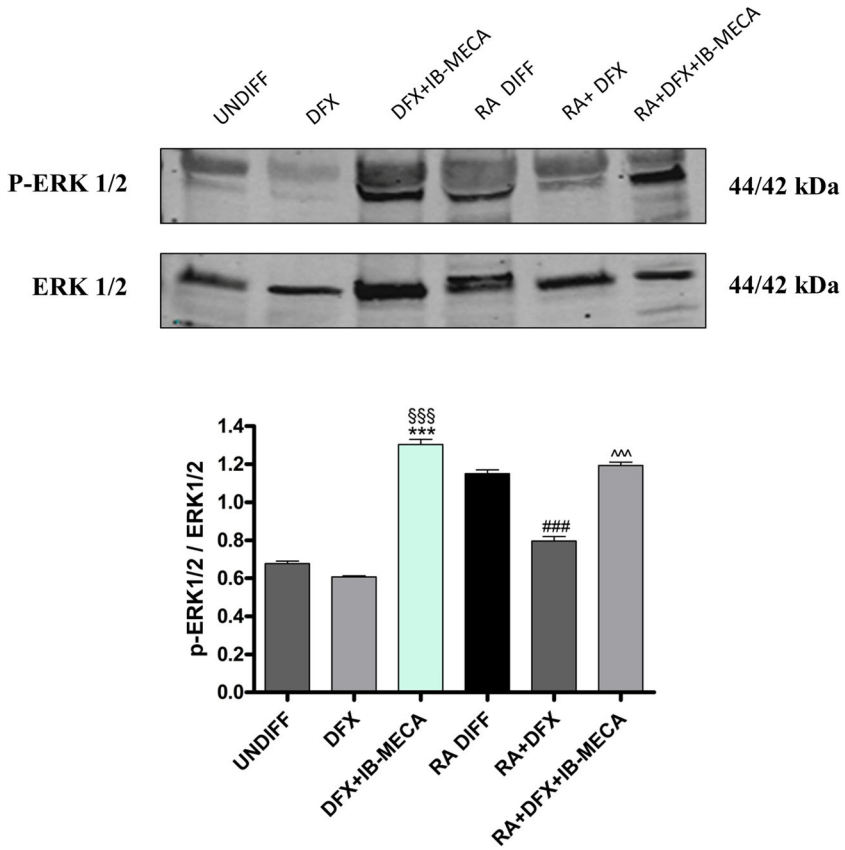

Fig. 7 A_3 adenosine receptor regulates the phosphorylation of ERK1/2 in RA-differentiated neuroblastoma cells exposed to hypoxia. Representative immunoblots of p-Erk1/2 expression in SH-SY5Y cells cultured in growth medium (UNDIFF) or added with 10 μM all-trans retinoic acid (RA DIFF) treated with 100 nM IB-MECA under hypoxic condition. The bar graphs show mean ± SEM of signals. Each signal of the phosphorylated protein was normalized to total protein expression. $^{***}p < 0.001$ vs UNDIFF; $^{§§§}p < 0.001$ vs DFX; $^{###}p < 0.001$ vs RA DIFF; $^{^^^}p < 0.001$ vs RA + DFX, as determined by one-way ANOVA followed by the Tukey post hoc test. Relative band densities were quantified by using the ImageJ software

3a, b). The latter could be considered an in vitro model of ganglioneuroma, representing the most benign form of neuroblastic tumors. In accord, nestin, a marker of malignancy, is drastically increased in undifferentiated NB cells confirming their high-grade aggressiveness (Fig. 2).

During tumor growth, hypoxic areas progress into the cancer mass as a response to low oxygen supply leading to tissue necrosis and neovascularization. Cellular microenvironment modifications lead to adenosine accumulation in tissue as a result of extracellular ATP metabolism (Layland et al. 2014; Fredholm 2007). Upregulation of this nucleoside is involved in a cellular response to hypoxia. In particular, increased level of this autacoid in extracellular fluid could have a key role in tumor growth by stimulating the hypoxic/angiogenic pathway (Leone and Emens 2018).

In accord, we have demonstrated that adenosine modulates this pathway in NB through stimulation of A_3 AR and this effect is more intense in undifferentiated than in differentiated cells.

In line with previous studies, our results have shown that in response to hypoxia, adenosine increases HIF-1α and HIF-2α expression in NB (Merighi et al. 2005, 2006). Moreover, this effect is A_3 AR-mediated since HIF-1α and HIF-2α expression is drastically increased or reduced treating cells with the A_3 AR agonist or antagonist, respectively (Fig. 4).

As previously argued, hypoxia increases the endothelial specific mitogen VEGF playing a key role in neovascularization of NB cells (Roy Choudhury et al. 2011). Our data showed that adenosine mediates angiogenesis through selective activation of A_3 AR leading to VEGF overexpression in undifferentiated and RA-differentiated NB cells exposed to hypoxia (Fig. 5).

Different reports have demonstrated that a hypoxia-driven VEGF autocrine loop is involved in NB cell proliferation, aggressiveness, and drug resistance (Das et al. 2005; Lim et al. 2004; Mottet et al. 2002). Furthermore, the MAPK-ERK1/2 pathway is required for the HIF overexpression induced by A_3 AR activation in human melanoma, glioblastoma, and colon cancer cells in response to hypoxia (Merighi et al. 2005, 2006). Here, we have demonstrated the direct involvement of A_3 AR activation in the hypoxic/angiogenic event in NB mediated by the MAPK-ERK1/2 pathway (Figs. 6 and 7).

Conclusion

To conclude, the overexpression as well as the ability to intensively trigger the hypoxic/angiogenic pathway in undifferentiated cells has suggested that A_3 AR may represent a marker or a therapeutic target of malignant NB useful for improving the clinical outcome of patients.

Compliance with Ethical Standards

Competing Interests The authors declare that they have no competing interests.

References

Andiné P, Rudolphi KA, Fredholm BB, Hagberg H (1990) Effect of propentofylline (HWA 285) on extracellular purines and excitatory amino acids in CA1 of rat hippocampus during transient ischaemia. Br J Pharmacol 100:814–818

Blay J, White TD, Hoskin DW (1997) The extracellular fluid of solid carcinomas contains immunosuppressive concentrations of adenosine. Cancer Res 57:2602–2605

D'Amico AG, Scuderi S, Maugeri G, Cavallaro S, Drago F, D'Agata V (2014) NAP reduces murine microvascular endothelial cells proliferation induced by hyperglycemia. J Mol Neurosci 54(3):405–413

D'Amico AG, Maugeri G, Magro G, Salvatorelli L, Drago F, D'Agata V (2015) Expression pattern of parkin isoforms in lung adenocarcinomas. Tumour Biol 36(7):5133–5141

D'Amico AG, Maugeri G, Bucolo C, Saccone S, Federico C, Cavallaro S, D'Agata V (2017) Nap interferes with hypoxia-inducible factors and VEGF expression in retina of diabetic rats. J Mol Neurosci 61(2): 256–266

Das B, Yeger H, Tsuchida R, Torkin R, Gee MF, Thorner PS et al (2005) A hypoxia-driven vascular endothelial growth factor/Flt1 autocrine loop interacts with hypoxia-inducible factor-1α through mitogen-activated protein kinase/extracellular signal-regulated kinase 1/2 pathway in neuroblastoma. Cancer Res 65(16):7267–7275

Epstein AC, Gleadle JM, McNeill LA, Hewitson KS, O'Rourke J, Mole DR, Mukherji M, Metzen E, Wilson MI, Dhanda A, Tian YM, Masson N, Hamilton DL, Jaakkola P, Barstead R, Hodgkin J, Maxwell PH, Pugh CW, Schofield CJ, Ratcliffe PJ (2001) C. elegans EGL-9 and mammalian homologs define a family of dioxygenases that regulate HIF by prolyl hydroxylation. Cell 107:43-54

Fredholm BB (2007) Adenosine, an endogenous distress signal, modulates tissue damage and repair. Cell Death Differ 14:1315–1323

Fredholm BB, Abbracchio MP, Burnstock G, Daly JW, Harden TK, Jacobson KA, Leff P, Williams M (1994) Nomenclature and classification of purinoceptors. Pharmacol Rev 46:143–156

Fredholm BB, IJzerman AP, Jacobson KA, Klotz KN, Linden J (2001) International Union of Pharmacology. XXV. Nomenclature and classification of adenosine receptors. Pharmacol Rev 53(4):527–552

Gessi S, Varani K, Merighi S, Morelli A, Ferrari D, Leung E, Baraldi PG, Spalluto G, Borea PA (2001) Pharmacological and biochemical characterization of A3 adenosine receptors in Jurkat T cells. Br J Pharmacol 134:116–126

Gessi S, Varani K, Merighi S, Cattabriga E, Iannotta V, Leung E, Baraldi PG, Borea PA (2002) A3 adenosine receptors in human neutrophils and promyelocytic HL60 cells: a pharmacological and biochemical study. Mol Pharmacol 61:415–424

Gessi S, Cattabriga E, Avitabile A, Gafa' R, Lanza G, Cavazzini L, Bianchi N, Gambari R, Feo C, Liboni A, Gullini S, Leung E, Mac-Lennan S, Borea PA (2004) Elevated expression of A3 adenosine receptors in human colorectal cancer is reflected in peripheral blood cells. Clin Cancer Res 10:5895–5901

Gessi S, Merighi S, Varani K, Cattabriga E, Benini A, Mirandola P, Leung E, Mac Lennan S, Feo C, Baraldi S, Borea PA (2007) Adenosine receptors in colon carcinoma tissues and colon tumoral cell lines: focus on the A3 adenosine subtype. J Cell Physiol 211:826–836

Gessi S, Sacchetto V, Fogli E, Merighi S, Varani K, Baraldi PG, Tabrizi MA, Leung E, Maclennan S, Borea PA (2010) Modulation of metalloproteinase-9 in U87MG glioblastoma cells by A3 adenosine receptors. Biochem Pharmacol 79:1483–1495

Hirsilä M, Koivunen P, Xu L, Seeley T, Kivirikko KI, Myllyharju J (2005) Effect of desferrioxamine and metals on the hydroxylases in the oxygen sensing pathway. FASEB J 19:1308-1310

Jajoo S, Mukherjea D, Watabe K, Ramkumar V (2009) Adenosine A3 receptor suppresses prostate cancer metastasis by inhibiting NADPH oxidase activity. Neoplasia 11:1132–1145

Keith B, Johnson RS, Simon MC (2011) HIF1α and HIF2α: sibling rivalry in hypoxic tumour growth and progression. Nat Rev Cancer 12(1):9–22

Layland J, Carrick D, Lee M, Oldroyd K, Berry C (2014) Adenosine: physiology, pharmacology, and clinical applications. JACC Cardiovasc Interv 7:581–591

Leone RD, Emens LA (2018) Targeting adenosine for cancer immunotherapy. J Immunother Cancer 6(1):57

Lim JH, Lee ES, You HJ, Lee JW, Park JW, Chun YS (2004) Ras-dependent induction of HIF-1alpha785 via the Raf/MEK/ERK pathway: a novel mechanism of Ras-mediated tumor promotion. Oncogene 23:9427–9431

Maugeri G, D'Amico AG, Rasà DM, Reitano R, Saccone S, Federico C, Parenti R, Magro G, D'Agata V (2016a) Expression profile of Wilms tumor 1 (WT1) isoforms in undifferentiated and all-trans retinoic acid differentiated neuroblastoma cells. Genes Cancer 7(1–2):47–58

Maugeri G, D'Amico AG, Reitano R, Magro G, Cavallaro S, Salomone S et al (2016b) PACAP and VIP inhibit the invasiveness of glioblastoma cells exposed to hypoxia through the regulation of HIFs and EGFR expression. Front Pharmacol 31(7):139

Maugeri G, D'Amico AG, Rasà DM, La Cognata V, Saccone S, Federico C et al (2017) Caffeine prevents blood retinal barrier damage in a model, in vitro, of diabetic macular edema. J Cell Biochem 118(8): 2371–2379

Maugeri G, D'Amico AG, Rasà DM, Saccone S, Federico C, Cavallaro S, D'Agata V (2018a) PACAP and VIP regulate hypoxia-inducible factors in neuroblastoma cells exposed to hypoxia. Neuropeptides. 69:84–91

Maugeri G, Longo A, D'Amico AG, Rasà DM, Reibaldi M, Russo A et al (2018b) Trophic effect of PACAP on human corneal endothelium. Peptides 99:20–26

Merighi S, Varani K, Gessi S, Cattabriga E, Iannotta V, Ulouglu C, Leung E, Borea PA (2001) Pharmacological and biochemical characterization of adenosine receptors in the human malignant melanoma A375 cell line. Br J Pharmacol 134:1215–1226

Merighi S, Mirandola P, Varani K, Gessi S, Leung E, Baraldi PG, Tabrizi MA, Borea PA (2003) A glance at adenosine receptors: novel target for antitumor therapy. Pharmacol Ther 100:31–48

Merighi S, Benini A, Mirandola P, Gessi S, Varani K, Leung E, MacLennan S, Baraldi PG, Borea PA (2005) A3 adenosine receptors modulate hypoxia-inducible factor1α expression in human A375 melanoma cells. Neoplasia 7:894–903

Merighi S, Benini A, Mirandola P, Gessi S, Varani K, Leung E, Maclennan S, Borea PA (2006) Adenosine modulates vascular endothelial growth factor expression via hypoxia-inducible factor-1 in human glioblastoma cells. Biochem Pharmacol 72:19–31

Merighi S, Benini A, Mirandola P, Gessi S, Varani K, Leung E, Maclennan S, Baraldi PG, Borea PA (2007) Hypoxia inhibits paclitaxel-induced apoptosis through adenosine-mediated

phosphorylation of BAD in glioblastoma cells. Mol Pharmacol 72: 162–172

Mottet D, Michel G, Renard P, Ninane N, Raes M, Michiels C (2002) ERK and calcium in activation of HIF-1. Ann N Y Acad Sci 973: 448–453

Murphy JM, La Quaglia MP (2014) Advances in the surgical treatment of neuroblastoma: a review. Eur J Pediatr Surg 24(6):450–456

Musumeci G, Castorina A, Magro G, Cardile V, Castorina S, Ribatti D (2015a) Enhanced expression of CD31/platelet endothelial cell adhesion molecule 1 (PECAM1) correlates with hypoxia inducible factor-1 alpha (HIF-1α) in human glioblastoma multiforme. Exp Cell Res 339(2):407–416

Musumeci G, Magro G, Cardile V, Coco M, Marzagalli R, Castrogiovanni P, Imbesi R, Graziano ACE, Barone F, di Rosa M, Castorina S, Castorina A (2015b) Characterization of matrix metalloproteinase-2 and -9, ADAM-10 and N-cadherin expression in human glioblastoma multiforme. Cell Tissue Res 362(1):45–60

Nakamura K, Yoshikawa N, Yamaguchi Y, Kagota S, Shinozuka K, Kunitomo M (2006) Antitumor effect of cordycepin (3-deoxyadenosine) on mouse melanoma and lung carcinoma cells involves adenosine A3 receptor stimulation. Anticancer Res 26: 43–47

Noguera R, Fredlund E, Piqueras M, Pietras A, Beckman S, Navarro S, Påhlman S (2009) HIF-1alpha and HIF-2alpha are differentially regulated in vivo in neuroblastoma: high HIF-1alpha correlates negatively to advanced clinical stage and tumor vascularization. Clin Cancer Res 15:7130–7136

Okamoto A, Sumi C, Tanaka H, Kusunoki M, Iwai T, Nishi K, Matsuo Y, Harada H, Takenaga K, Bono H, Hirota K (2017) HIF-1-mediated suppression of mitochondria electron transport chain function confers resistance to lidocaine-induced cell death. Sci Rep 7:3816

Påhlman S, Mohlin S (2018) Hypoxia and hypoxia-inducible factors in neuroblastoma. Cell Tissue Res 372:269–275

Qiao J, Paul P, Lee S, Qiao L, Josifi E, Tiao JR, Chung DH (2012) PI3K/AKT and ERK regulate retinoic acid-induced neuroblastoma cellular differentiation. Biochem Biophys Res Commun 424(3):421–426

Roy Choudhury S, Karmakar S, Banik NL, Ray SK (2011) Targeting angiogenesis for controlling neuroblastoma. J Oncol 2012:782020

Semenza GL (2003) Targeting HIF-1 for cancer therapy. Nat Rev Cancer 3(10):721–732

Semenza GL (2014) Oxygen sensing, hypoxia-inducible factors, and disease pathophysiology. Annu Rev Pathol 9:47–71

Suh BC, Kim TD, Lee JU, Seong JK, Kim KT (2001) Pharmacological characterization of adenosine receptors in PGT-beta mouse pineal gland tumor cells. Br J Pharmacol 134:132–142

Torres Á, Erices JI, Sanchez F, Ehrenfeld P, Turchi L, Virolle T, Uribe D, Niechi I, Spichiger C, Rocha JD, Ramirez M, Salazar-Onfray F, San Martín R, Quezada C (2019) Extracellular adenosine promotes cell migration/invasion of glioblastoma stem-like cells through A3 adenosine receptor activation under hypoxia. Cancer Lett 446:112–122

Whittle SB, Smith V, Doherty E, Zhao S, McCarty S, Zage PE (2017) Overview and recent advances in the treatment of neuroblastoma. Expert Rev Anticancer Ther 17(4):369–386

Wigerup C, Påhlman S, Bexell D (2016) Therapeutic targeting of hypoxia and hypoxia-inducible factors in cancer. Pharmacol Ther 164:152–169

Yao Y, Sei Y, Abbracchio MP, Jiang JL, Kim YC, Jacobson KA (1997) Adenosine A3 receptor agonists protect HL-60 and U-937 cells from apoptosis induced by A3 antagonists. Biochem Biophys Res Commun 232:317–322

Yegutkin GG (2014) Enzymes involved in metabolism of extracellular nucleotides and nucleosides: functional implications and measurement of activities. Crit Rev Biochem Mol Biol 49:473–497